Proceedings of the International Workshop "Oxide Materials for Electronic Engineering" (OMEE-2009), Lviv 2009

Luminescence and Luminescence Kinetics of $Gd_3Ga_5O_{12}$ Polycrystals Doped with Cr^{3+} and Pr^{3+}

S. Mahlik, B. Kukliński, M. Grinberg*

Institute of Experimental Physics, University of Gdańsk, Wita Stwosza 57, 80-952 Gdańsk, Poland

L. Kostyk and O. Tsvetkova

Faculty of Electronics, Ivan Franko Lviv National University, Tarnovskovo 107, 79017 Lviv, Ukraine

In this paper spectroscopic investigations of $Gd_3Ga_5O_{12}$ (GGG) polycrystals, containing Cr^{3+} and intentionally doped with Pr^{3+} of concentrations 0.5, 1 and 1.5 mol% are presented. We have measured the steady state luminescence and luminescence excitation spectra, as well as the time resolved spectra and luminescence kinetics. The main goal was to investigate the excitation energy transfer from lattice to impurity and between impurities. We found that relative intensity of Cr^{3+} and GGG lattice luminescence decreased when material was doped with Pr^{3+}. On the other hand, time resolved spectroscopy and luminescence decay measurements showed that the Cr^{3+} and GGG lattice luminescence decays were independent of Pr^{3+} content. The lifetime of Pr^{3+} luminescence related to $^1D_2 \rightarrow {}^3H_4$ and $^3P_0 \rightarrow {}^3H_4$ transitions decreased with concentration of Pr^{3+}, which was attributed to the concentration luminescence quenching. No energy transfer between GGG lattice defects and Cr^{3+}, and Pr^{3+} ions was observed. We proposed the model of radiative recombination of electron and hole, which took place through three independent pathways: by GGG host emission that peaked at 12750 cm^{-1}, by Cr^{3+} luminescence that peaked at 15400 cm^{-1}, and by Pr^{3+} luminescence.

PACS numbers: 78.55.Hx, 78.60.Kn, 78.70.En

1. Introduction

The gadolinium gallium garnet crystals $Gd_3Ga_5O_{12}$ (GGG) doped with RE^{3+} (RE = rare earth) ions are interesting materials for solid state lasers. The laser action has been reported in GGG:Nd^{3+}, in the spectral range 1.06–1.42 μm [1, 2] and in GGG:Yb^{3+}, in the spectral range 1.048 μm [3–5]. The GGG crystals doped with various rare-earth ions (Eu^{3+}, Pr^{3+}, Tb^{3+}, Er^{3+} [6] and Tm^{3+}, and Yb^{3+} [7]) have been also used for demonstration of up-conversion processes. GGG doped with Cr^{3+} and rare earth have been used as scintillation and dosimetric materials [8]. Above applications caused the direction of the research focused on nature of luminescence and mechanisms of the excitation energy transfer from lattice to luminescence centers.

In this paper spectroscopic investigations of GGG polycrystals, containing Cr^{3+} and intentionally doped with Pr^{3+} of concentration 0.5, 1 and 1.5 mol%, are presented. We measured the steady state luminescence and luminescence excitation spectra, as well as the time resolved spectra and luminescence kinetics. The main goal was to investigate the excitation energy transfer from lattice to impurity and between impurities.

* corresponding author; e-mail: fizmgr@univ.gda.pl

2. Experimental

The ceramic samples were prepared by standard ceramic technology such as high temperature solid-state synthesis. High-purity powders of Ga_2O_3 and Gd_2O_3 (99.999% purity on a caution basis) were used as starting materials. The impurities were entered as Pr_2O_3 oxide (99.99%). The content of Pr impurity varies from 0.5 to 1.5 mol%. Oxide powders were mechanically mixed in agate mortar till receipt of homogeneous mass. Pellets were formed by uniaxial pressing of the powders in a steel die (8 mm in diameter) at 150 kg/cm^2 and heated for 10–12 h at 1200 °C.

Powder X-ray diffraction (XRD) was carried out at room temperature on a STOE STADI P diffractometer with the Bragg–Brentano geometry using Cu K_α radiation. The diffraction peaks of the powder were identified as $Cd_3Ga_5O_{12}$ phase. XRD pattern of the sample is shown in Fig. 1. All of the observed peaks are characteristic of $Cd_3Ga_5O_{12}$ garnet phase and no other phases are detected. The details of GGG synthesis have been described in [9, 10].

The experimental setup for luminescence kinetics and time resolved spectra consists of YAG:Nd laser system PL 2143 A/SS and the parametric optical generator PG 401/SH that generates 30 ps pulses, with frequency 10 Hz, in spectral range from 210 to 2700 nm.

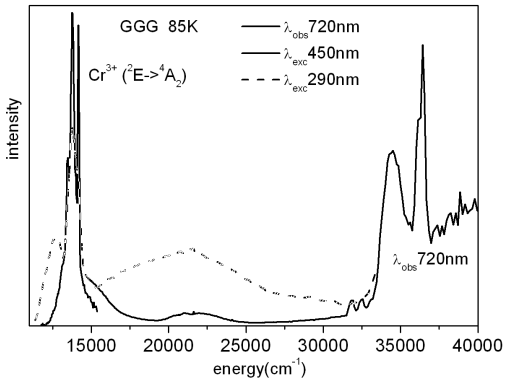

Fig. 1. Luminescence spectra and luminescence excitation spectra (solid curve) of GGG ceramics containing Cr^{3+} ions at liquid nitrogen temperature. Luminescence excited with 290 nm is presented by dashed curve. Luminescence excited with 450 nm (22200 cm^{-1} is presented by dashed-dotted curve.

The detection part consists of the spectrograph 2501S (Bruker Optics) and the Hamamatsu Streak Camera model C4334-01. The time resolved luminescence spectra were collected by integration of the streak camera pictures over the time intervals, whereas the luminescence decays were collected by integration of the streak camera pictures over the wavelength intervals.

Luminescence excitation spectra and steady state emission spectra were measured using a system consisting of a Xe lamp (450 W), two monochromators SPM2 (one in the excitation and one in the detection line) and two photomultipliers (the first for the luminescence and the second for reference signal detection). All spectra were corrected for instrumental response. The same apparatus has been used to obtain the integrated spectra.

3. Results and discussion

The luminescence and luminescence excitation spectra obtained at liquid nitrogen temperature are presented in Fig. 1. One notices that at low temperature the luminescence band that at room temperature peaked at 13900 cm^{-1} appeared to consist of three sharper bands peaked at 13700 cm^{-1}, 13770 cm^{-1}, 14170 cm^{-1} (dashed curve). Additionally, one noticed that this luminescence can be effectively excited in the region 22200 cm^{-1} (450 nm) and 15400 cm^{-1} (650 nm). The respective excitation spectrum is presented by solid curve in Fig. 1. Luminescence excited with 450 nm is presented by solid curve. The structure of the low temperature emission with peaks at 13700 cm^{-1}, 13770 cm^{-1}, 14170 cm^{-1} corresponded to the luminescence of Cr^{3+} related to spin forbidden $^2E \rightarrow {}^4A_2$ transition accompanied by phonons induced side band, observed in Cr^{3+} doped GGG polycrystal [8]. Thus the excitation bands peaked at 22200 cm^{-1} (450 nm) and 15400 cm^{-1} (650 nm) can be related to $^4A_2 \rightarrow {}^4T_1$ and $^4A_2 \rightarrow {}^4T_2$ transitions in Cr^{3+} ions. The Cr^{3+} ions appeared in the GGG ceramic as the unintended impurity with low, uncontrolled content. Under excitation with 34500 cm^{-1} (290 nm) one obtained additional band peaked at 12650 cm^{-1} (dashed curve) and very broad luminescence extended from 15000 to 30000 cm^{-1} and peaked at 21000 cm^{-1} (475 nm) was observed. We related the emission peaked at 12650 cm^{-1} to the GGG host emission and emission peaked at 21000 cm^{-1} to F centers, formed by complex ($V_{Ga}V_O$) [11]. The luminescence excitation spectrum for higher energy consisted of relatively sharp lines peaked at 31845 cm^{-1} and 32495 cm^{-1}, related to $^8S_{7/2} \rightarrow {}^6P_{7/2}$ and $^8S_{7/2} \rightarrow {}^6P_{5/2}$ transitions in Gd^{3+} ion, and two broad bands peaked at 34500 cm^{-1} and 37000 cm^{-1}. The excitation band peaked at 34500 cm^{-1} has been considered as the related to absorption Ga vacancy and oxygen vacancy complex ($V_{Ga}V_O$) [11]. The band gap of GGG crystal has been calculated and equals 4.03 eV (32500 cm^{-1}) [12]. It is known that for insulator calculated value of band gap obtained using local density approximation (LDA) is usually underestimated by 25–30%, therefore we considered that band peaked at 37000 cm^{-1} in excitation spectrum can be related to band-to-band transition.

The luminescence spectra of GGG ceramic "pure" and doped with Pr^{3+} with concentrations 0.1, 0.5, 1.0 and 1.5 mol%, excited with wavelength 280 nm are presented in Fig. 2. The spectra were superpositions of the broad band related mainly to host emission and Cr^{3+} emission, and sharp lines related to transitions from $^3P_0$, $^3P_1$ and $^1D_2$ states of Pr^{3+} ion. One noticed that intensity of lattice luminescence decreased with increase of Pr^{3+} content.

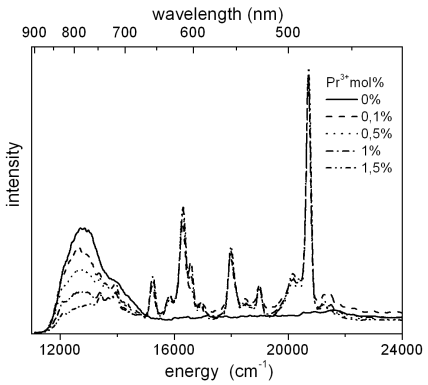

Fig. 2. Luminescence spectra of GGG ceramics without Pr^{3+} and doped with Pr3+ with different mole concentrations labeled in Figure. Luminescence was excited at 280 nm.

In Fig. 3a the luminescence spectra of GGG:Pr^{3+} with Pr^{3+} of 1 mol%, excited with 450 nm, obtained at room temperature and liquid nitrogen temperature are presented. The individual spectral lines of Pr^{3+} f–f emission were attributed to the respective transitions from $^3P_0$ and $^1D_2$ states. It was seen that the spectra were dominated by transitions from the $^3P_0$ state that

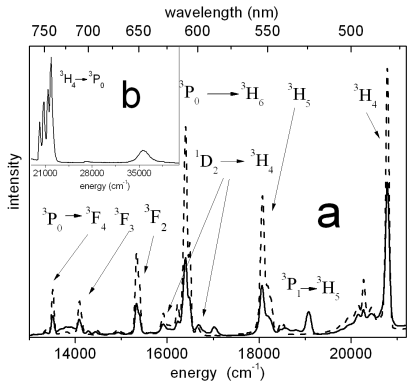

Fig. 3. (a) Luminescence of GGG:Pr^{3+} with concentration of Pr^{3+} 1 mol%, at room temperature (solid curve) and at liquid nitrogen temperature (dashed curve), excited with 450 nm (22200 cm^{-1}). (b) Excitation spectra of $^3P_0 \rightarrow {}^3H_6$ luminescence monitored at 16400 cm^{-1}, obtained at room temperature.

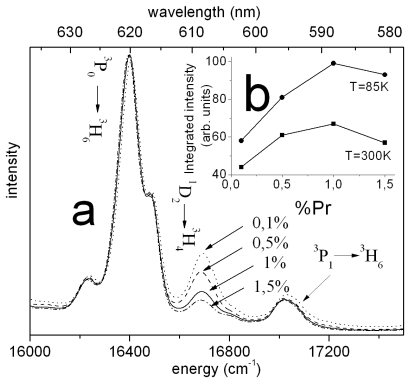

Fig. 4. (a) The relative intensity of the $^3P_0 \rightarrow {}^3H_6$ and $^1D_2 \rightarrow {}^3H_4$ transition in GGG:Pr^{3+} with different concentrations of Pr^{3+}. (b) Total integrated intensity of the whole Pr^{3+} emission at liquid nitrogen and room temperature are presented. Luminescence was excited at 450 nm.

is higher excited state of Pr^{3+}. In Fig. 3b the luminescence excitation spectrum (luminescence was monitored at 16400 cm^{-1} ($^3P_0 \rightarrow {}^3H_6$ transition)) obtained at room temperature is presented. The spectrum consisted of sharp lines related to $^3H_4 \rightarrow {}^3P_0$ transition at 21000 cm^{-1} and band peaked at 35500 cm^{-1} that can be related to complex ($V_{Ga}V_O$) or charge transfer transition.

The intensity of the luminescence originating from $^1D_2$ state decreased with respect to the intensity of emission from $^3P_0$ state when concentration of praseodymium in the material increased. This effect is seen in Fig. 4a, where luminescence related to the $^1D_2 \rightarrow {}^3H_4$ and $^3P_0 \rightarrow {}^3H_6$ transitions obtained for the different concentration of Pr^{3+} are presented. The spectra presented in Fig. 4 are normalized to the maximum intensity of $^3P_0 \rightarrow {}^3H_6$ emission. Since the luminescence was measured under the same conditions, one can consider the integrated luminescence intensity as proportional to the luminescence efficiency of the system. These quantities are presented in Fig. 4b. One can notice that the sample with 1 mol% of Pr^{3+} was characterized by highest luminescence efficiency.

Time resolved luminescence spectra of GGG and GGG doped with 1 mol% of Pr^{3+} are presented in Fig. 5. The spectra of GGG without Pr^{3+} and GGG:Pr^{3+} are presented by dashed and solid curves, respectively. The spectra changed with time. At time range 0–200 μs after pulse the emission of GGG consists of broad band with main peak at 13900 cm^{-1} (related to Cr^{3+} luminescence) and the bump peaked at 12900 cm^{-1}, related to GGG host emission. At the time scale 0.2–1 ms the spectrum is a superposition of two bands: the stronger peaked at 12850 cm^{-1} and the weaker peaked at 13850 cm^{-1}. In the time scale 1–10 ms only single band is observed that peaked at 12750 cm^{-1}.

At time range 0–200 μs the luminescence of GGG:Pr^{3+} was dominated by transitions from the higher excited

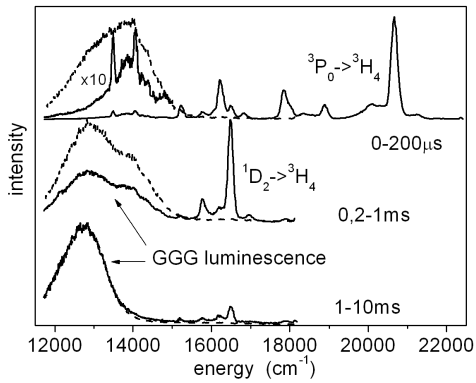

Fig. 5. Room temperature time resolved spectra of GGG (dashed curves) and GGG:Pr^{3+} with concentration of Pr^{3+} (0.5 mol%) excited with wavelength 280 nm.

state of Pr^{3+}; $^3P_0$. At time scale 0.2–1 ms the luminescence consisted of broad brad band peaked at 12850 cm^{-1} (GGG lattice emission), smaller band peaked at 13900 cm^{-1} (Cr^{3+} luminescence) and sharp lines related to $^1D_2 \rightarrow {}^3H_4$ transition. At time range 1–10 ms the spectrum is dominated by broad band related GGG luminescence peaked at 12750 cm^{-1}.

The decays of the luminescence monitored at spectral range 12000–15000 cm^{-1} are presented in Fig. 6a and b. Figure 6a contains emission decays measured in the time scale 0–10 ms. In Fig. 6b the emission decays measured in the time interval 0–1 ms are presented. The decays were decomposed into two exponents according to relation

$$I(t) = A_1 \exp\left(\frac{-t}{\tau_1}\right) + A_2 \left(\frac{-t}{\tau_2}\right). \quad (1)$$

Calculations were performed independently for all considered samples, and the results are presented in Table. The average decay constants were calculated and assumed

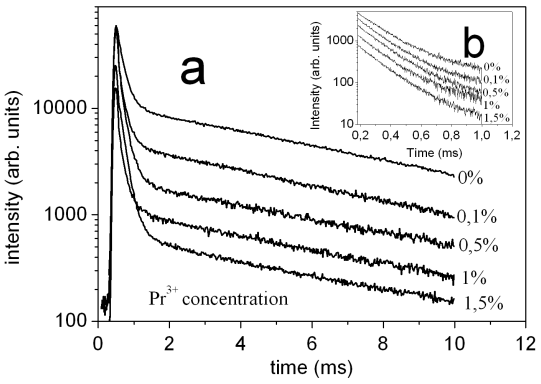

Fig. 6. (a) Luminescence decay profiles of the GGG:Pr^{3+} emission for luminescence monitored at spectral region 12000–13000 cm^{-1} band, for different concentrations of Pr^{3+} for excitation 280 nm. (b) The emission decays measured in the time interval 0–1 ms are presented.

to represent the lifetimes of two luminescence centers of GGG. Decay constant, 0.169 ± 0.003 ms, was attributed to Cr^{3+} luminescence whereas 6.48 ± 0.07 ms decay constant was attributed to the GGG host emission. No correlations between decay constants and concentration of Pr^{3+} were observed. Time evolution of the luminescence showed that Cr^{3+} emission and GGG host emission decayed independently with two different decay constants. This effect led to conclusion that there was no excitation energy transfer between the GGG luminescence center and Cr^{3+}. The independence of lattice luminescence kinetics of Pr^{3+} provided the argument for the lack of energy transfer between the centers responsible for GGG lattice emission and Pr^{3+} ions. Thus GGG:Pr^{3+} excited with 270–290 nm relaxed either to Pr^{3+} or to GGG luminescence centers, or to Cr^{3+}.

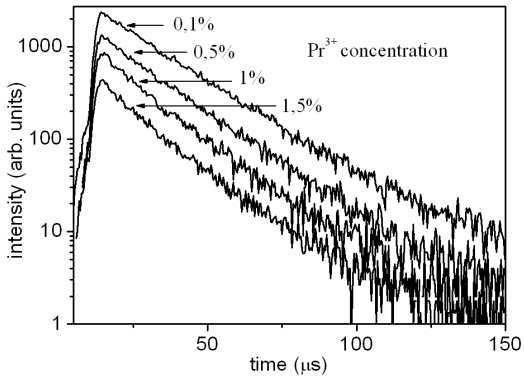

Fig. 7. Luminescence decay profiles of the $^3P_0 \rightarrow {}^3H_4$ transition obtained for GGG:Pr^{3+} for different concentrations of Pr^{3+} under pulse excitation 280 nm.

TABLE

The decays of the luminescence monitored at spectral range 12000–14000 cm^{-1} after excitation with 280 nm.

	A_1	τ_1 [ms]	A_2	τ_2 [ms]	$A_1/(A_1+A_2)$	$A_2/(A_1+A_2)$
GGG	30331	0.175	10250	6.47	0.75	0.25
GGG:Pr(0.1%)	17296	0.168	4585	6.26	0.79	0.21
GGG:Pr(0.5%)	19054	0.164	2054	6.64	0.90	0.10
GGG:Pr(1%)	4335	0.162	1075	6.52	0.80	0.20
GGG:Pr(1.5%)	9760	0.174	620	6.49	0.94	0.06
average lifetimes		0.169 ± 0.003		6.48 ± 0.07		

Decays of the luminescence related to $^3P_0 \rightarrow {}^3H_4$ transition monitored at 20500–20800 cm^{-1} are presented in Fig. 7. It was found that for all Pr^{3+} concentrations luminescence decays almost exponentially with the lifetime that slightly decreased with increasing praseodymium concentration. We calculated the average lifetime according to the formula

$$\tau = \frac{\int t \cdot I(t)\,\mathrm{d}t}{\int I(t)\,\mathrm{d}t} \qquad (2)$$

and obtained 22 μs, 20 μs and 18 μs for concentrations of Pr^{3+} 0.1, 05 and 1, and 1.5 mol%, respectively.

Luminescence decays of the emission related to $^1D_2 \rightarrow {}^3H_4$ transition are presented in Fig. 8. Similarly like for $^3P_0 \rightarrow {}^3H_4$ emission the $^1D_2 \rightarrow {}^3H_4$ luminescence decayed almost exponentially with the lifetime that decreased with increasing praseodymium concentration. We calculated the average lifetime according to the formula (2) and obtained 165 μs, 153 μs, 113 μs and 99 μs for Pr^{3+} concentrations equal to 0.1, 0.5, 1.0, and 1.5 mol%, respectively.

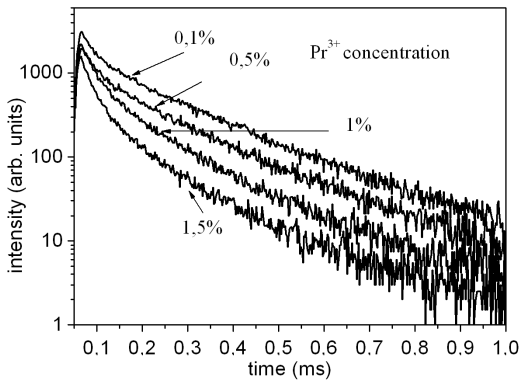

Fig. 8. Luminescence decay profiles of the $^1D_2 \rightarrow {}^3H_4$ transition obtained for GGG:Pr^{3+} for different concentrations Pr^{3+} under pulse excitation 280 nm.

4. Conclusions

Luminescence of GGG and GGG doped with Pr^{3+} was measured. The GGG lattice luminescence band with peak at 12650 cm^{-1} and excitation peaked at 37000 cm^{-1} (270 nm) was measured and was characterized by lifetime equal to 6.48 ± 0.07 ms. Time resolved spectra showed that GGG lattice luminescence is observed also when material was doped with Pr^{3+}. The large Stokes shift between absorption and emission of lattice luminescence suggested that the GGG lattice luminescence was created by excitation of free hole or/and electron in the bands. The GGG lattices luminescence decreased when material was doped with Pr^{3+}. This effect was not accompanied by diminishing of their lifetimes. Luminescence band in the spectral region 13700–14200 cm^{-1} characterized by excitation bands peaked at 34500 cm^{-1} (290 nm), 22200 cm^{-1} (450 nm) and 15400 cm^{-1} (650 nm), and lifetime equal to 0.169 ± 0.03 ms was related to Cr^{3+} luminescence. Pr^{3+} luminescence related to $^1D_2 \rightarrow {}^3H_4$ and $^3P_0 \rightarrow {}^3H_4$ transitions was observed, and the respective luminescence lifetimes decreased with concentration of Pr^{3+}, which was attributed to the concentration luminescence quenching. After excitation with wavelength shorter than 290 nm the GGG:Pr^{3+} relaxed either by GGG lattice defects luminescence or by Cr^{3+}, or by Pr^{3+} luminescence. No energy transfer between GGG lattice defects and Cr^{3+}, and Pr^{3+} ions was observed. This allowed to conclude that radiative recombination of electron and hole took place through three independent pathways: by GGG host emission that peaked at 12750 cm^{-1}, by Cr^{3+} luminescence that peaked at 15400 cm^{-1} and by Pr^{3+} luminescence. The emission related to recombination through the F centers is weak when material is doped with Pr^{3+}.

Acknowledgments

This paper has been supported by grant of Polish Ministry of Science and Higher Education in years 2008–2011.

References

[1] M. Doroshenko, V. Osiko, V. Sigachev, M. Timoshechkin, *Sov. J. Quant. Electron.* **21**, 724 (1991).

[2] M. Doroshenko, V. Osiko, V. Sigachev, M. Timoshechkin, *Sov. J. Quant. Electron.* **23**, 490 (1993).

[3] Y. Guyot, H. Canibano, C. Goutaudier, A. Novoselov, A. Yoshikawa, T. Fukuda, G. Boulon, *Opt. Mater.* **28**, 1 (2006).

[4] S. Chéenais, F. Druon, F. Balembois, P. Georges, A. Brenier, G. Boulon, *Opt. Mater.* **22**, 99 (2003).

[5] Y. Guyot, H. Canibano, C. Goutaudier, A. Novoselov, A. Yoshikawa, T. Fukuda, G. Boulon, *Opt. Mater.* **27**, 1658 (2005).

[6] F. Pandozzi, F. Vetrone, J.-C. Boyer, R. Neccache, J.A. Capobianco, A. Speghini, M. Bettinelli, *J. Phys. Chem. B* **109**, 17400 (2005).

[7] Maolin Pang, Jun Lin, *J. Cryst. Growth* **248**, 262 (2005).

[8] L. Kostyk, A. Luchechko, Ya. Zakharko, O. Tsvetkova, B. Kukliński, *J. Lumin.* **129**, 312 (2009).

[9] E.E. Hellstrom, R.D. Ray II, C. Zhang, *J. Am. Ceram. Soc.* **72**, 1376 (1989).

[10] G. Blasse, B.C. Grabmaier, M. Ostertag, *J. Alloys Comp.* **200**, 17 (1993).

[11] V.I. Vasyltsiv, Ya.M. Zakharko, A.O. Matkovskii, D.Yu. Sugak, S.B. Ubizskii, Ya.I. Rym, A. Yu. Gavrilyuk, *Phys. Status Solidi A* **140**, 353 (1993).

[12] Yong-Nian Xu, W.Y. Ching, *Phys. Rev. B* **61**, 1817 (2000).